Hematological Response of Topotecan in Tumor-Bearing Rats: Modeling of the Time Course of Different Cellular Populations

Cristina Segura,[1] Eva Bandrés,[2] Iñaki F. Trocóniz,[1] Jesús García-Foncillas,[2] Onintza Sayar,[1] Carmen Dios-Vieítez,[1] Mª Jesús Renedo,[1] and María J. Garrido[1,3]

Received November 5, 2003; accepted December 5, 2003

Purpose. To evaluate the hematotoxicity of topotecan (TPT) in tumor-bearing rats by a pharmacokinetic/pharmacodynamic approach.
Methods. DHD/K12-PROb cells were subcutaneously injected in syngenic BD-IX rats. Three weeks after implantation of cells, animals received saline or 6 mg/kg i.p. dose of TPT (group II). Thirty days later, group II was divided into groups IIA receiving a single administration of 6 mg/kg and IIB treated with 3 mg/kg for 2 consecutive days. Leukocytes, neutrophils, and mature lymphocytes were measured in peripheral blood every 48 h for 45 days after first drug administration. Pharmacokinetic characteristics of TPT were also explored.
Results. Disposition of TPT in plasma was best described with a two-compartment model. A semiphysiological model discriminating between system-related and drug-effects parameters, such as the mean cell maturation or transition time (MTT) and the linear concentration-dependent inhibitory effects on cell proliferation (Slp), described adequately the time course of hematotoxicity. The estimates of MTT and Slp for the three cell populations ranged from 1.89 to 2.18 days and from 0.01 to 0.039 ml/ng, respectively.
Conclusion. The time course of the hematotoxicity induced after two cycles of chemotherapy with TPT in tumor-bearing rats could be described by a semiphysiological model.

KEY WORDS: hematotoxicity; pharmacokinetic–pharmacodynamic modeling; topotecan; tumor-bearing rats.

INTRODUCTION

Topotecan (TPT; Hycamtin®), approved in 1996 for the treatment of ovarian cancer, is a semisynthetic water-soluble analog of camptothecin (CPT) (1). TPT binds to topoisomerase I (topo-I), an essential enzyme in the replication of DNA, forming a cleavable complex (DNA–topo-I) that leads to an inhibition of cell division and consequently to cell death (2). TPT has a α-hydroxy-δl-lactone ring that undergoes reversible pH-dependent hydrolysis forming a carboxylate structure. Lactone form is responsible for the biological activity and predominates under acidic conditions (pH < 4), whereas the carboxylate form is inactive and predominates in physiological conditions of pH. The effectiveness of TPT treatment will depend on the lactone form concentration at the effect site (2,3).

In recent decades, several studies with TPT and irinotecan (CPT-11) have been conducted with positive results in the treatment of different types of cancer including colorectal cancer (3–5). Colorectal cancer represents 13% of all cancer in the world and has a high incidence of metastatic processes, 5 years being the survival time for 50–60% of the patients (6). For this reason, an active research activity involving the optimization of dosing schedules and routes of administration by exploring different drug delivery systems and a better molecular characterization of prognostic factors is currently taking place (7–9).

Preclinical research integrating pharmacokinetic/pharmacodynamic (pk/pd) modeling is expected to contribute in a significant manner to the understanding of the *in vivo* drug effects (10,11). Unfortunately, in the area of cancer, few studies have used this approach. Therefore, in the current study, an *in vivo* model with BD-IX rats bearing colon tumor has been developed to explore the hematological effects of TPT. Among others, Friberg *et al.* (12,13) have showed that continuous pd modeling can be used to describe the entire course of hematotoxicity induced by anticancer agents in both animals and humans; in addition, Mould *et al.* (14) have shown a clear relationship between neutropenia and TPT exposure in humans.

In the current study, the modeling of the time course of mature lymphocytes has also been considered because they are associated with the specific immune response, whereas the myeloid components are more related to the unspecific immune status. Results from Nygaard and Løvik (15) showed that lymphocytes from rat peripheral blood were a sensitive indicator of immunotoxic effects.

MATERIALS AND METHODS

Cell Culture

DHD/K12PROb cell line obtained from a colon adenocarcinoma induced in syngenic BD-IX rats was used in this study. Cells were cultured in monolayers in a mixture of Dulbecco's modified Eagle's medium and Ham's F-10 medium (1:1, v/v; GIBCO, BRL Life Technologies, Paisley, Scotland) supplemented with 10% fetal bovine serum (GIBCO BRL) and gentamicin (0.01%; GIBCO BRL).

Cells were trypsinized, washed, and resuspended in phosphate-buffered saline (PBS) just before injection into animals.

Animals and Drug Administration

Twenty-four male BD-IX rats (CRIFFA, Barcelona, Spain) weighing 300 ± 25 g were used. Groups of two animals were housed in microisolator cages under positive-pressure

[1] Department of Pharmacy and Pharmaceutical Technology, Faculty of Pharmacy, University of Navarra, Pamplona, Spain.
[2] Laboratory of Biotechnology, University Clinic, University of Navarra, Pamplona, Spain.
[3] To whom correspondence should be addressed. (e-mail: mgarrido@unav.es)

ABBREVIATIONS: $Circ_0$, absolute number of cells at baseline; CV, coefficient of variation; γ, slope parameter defining the rebound effect; IAV, inter-animal variability; k_{TR}, first-order rate constant governing the link between transit compartments; MTT, mean transit time; OBJF, minimum value of the objective function; RSE, relative standard error; Slp, slope parameter accounting for the inhibitory effects of TPT on the rate of synthesis of precursor cells; TPT, topotecan.

0724-8741/04/0400-0567/0 © 2004 Plenum Publishing Corporation

ventilation and maintained in closed-shelf, laminar-flow racks to avoid contact with pathogens, odors, or noises of other animals. All animals were kept under standard laboratory conditions. Sterilized food and water were available *ad libitum*. During the time of the experiments, the test for Mycoplasma pulmonis, *Salmonella* sp, Sendai virus, Hantaan virus, and Tooland H1 virus were performed on two animals used as control of the colony.

To induce the tumor, 250 μl of PBS containing 1×10^6 DHD/K12-PROb cells were subcutaneously injected into the right side of the chest in all animals (16). Tumor growth was weekly monitored by measurement of the external diameters with calipers. Body weights were recorded daily.

Three weeks after cells injection, animals were randomly divided into two groups: group I or control group (n = 11) receiving a physiological saline (pH 3) solution and group II or treated group (n = 13) receiving a 6 mg/kg dose of TPT. Thirty days after the first administration, animals from group II were randomly divided to receive a second treatment: group IIA (n = 6) received 6 mg/kg of TPT and group IIB (n = 6) was treated with 3 mg/kg of TPT for two consecutive days (Fig. 1).

Saline and TPT solutions were administered i.p. TPT was daily prepared using a sterile saline solution adjusted to pH = 3. The protocol of the study was approved by the Animal Experimentation Committee of the University of Navarra.

Hematological Response

To measure the hematological response, several blood samples were collected at different times during the study: before the first saline or TPT administration (baseline) and at different days after. Blood (250 μl) was collected in EDTA-prepared tubes from the retro-orbital sinus with animals lightly anesthetized (17) and used to quantify leukocyte, granulocyte, monocyte and lymphocyte levels. In group I, blood samples were collected every 3 or 4 days for 28 days after saline administration. Because 28 days was considered enough time to capture the tendency of the untreated hematological response, additional sampling was not performed to avoid suffering in the animals. In group II, blood samples were taken every 2 days during the first cycle of TPT, starting on day 1, the day after drug injection, in half of the animals and 1 day later in the other half, for 30 days. The same procedure was followed for 14 days in groups IIA and IIB after the second dose of TPT. Then, blood collection was stopped, but all animals were kept alive to explore tumor growth.

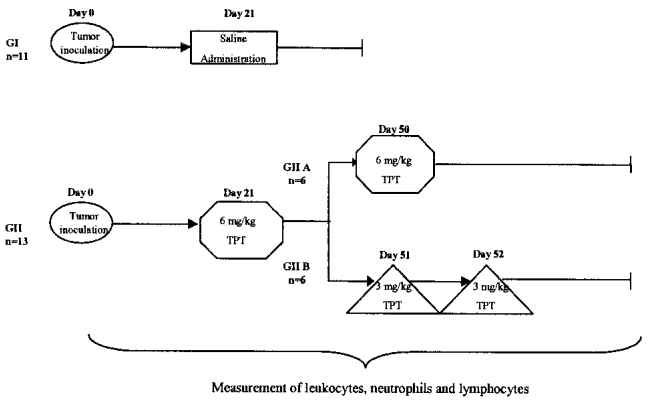

Fig. 1. Experimental design used in the current study. TPT and saline were given i.p. to tumor-bearing rats. Measurements of leukocytes, neutrophils, and lymphocytes were recorded throughout the study.

Leukocyte counts were determined in a Coulter Micro-Diff II Analyser (Coulter Corp., Hialeah, FL, USA) within 3 h of blood extraction. Lymphocyte, monocyte, and granulocyte populations were analyzed using a whole-blood lysis method (18). Red cells were lysed using FACS Lysing Solution (Becton-Dickinson, San Jose, CA, USA) and washed twice with PBS. Samples were analyzed using a Becton-Dickinson FACScan flow cytometer. Twenty-five thousand events were acquired, and dead cells and debris were excluded from the analysis by selective gating based on forward- and side-scatter parameters. For the analysis of blood leukocyte subsets, analysis regions were set in forward- and side-scatter patterns to separate events in three major populations of cells: lymphocytes, monocytes, and granulocytes. Moreover, CD90 expression was evaluated within the lymphocyte subpopulation to identify mature lymphocytes. Briefly, 100 μl of whole blood was added to tubes containing 10 μl of R-Phycoerytrin (R-PE)-conjugated mouse anti-rat CD90 (Thy-1) monoclonal antibody (Becton-Dickinson) and incubated for 15 min. Following incubation, red cells were lysed using FACS Lysing Solution, and the expression for the cell-surface antigen CD90 was analyzed gating the region of lymphocytes and represented as an FL2 histogram. We included labeled cells with isotype-matched irrelevant monoclonal antibody as a control. Absolute cell numbers for each specific subset were calculated on the basis of total leukocyte number.

Pk of TPT

The kinetic behavior of TPT in plasma was evaluated in a separate group of eight BD-IX male rats, following the same experimental procedure as is described above for groups II and IIA, B (Fig. 1).

Three weeks after tumor cells injection, 6 mg/kg of TPT were i.p. given and six blood samples were taken from each animal at specific times over a period of 5 h after drug administration. Thirty days after the first TPT dose, the eight animals were divided at random into two groups receiving i.p. a dose of 6 mg/kg or 3 mg/kg for 2 consecutive days. After the second and third TPT administration, six blood samples were taken from each animal for 5 h after drug administration.

To determine TPT lactone from plasma concentrations, blood samples were centrifuged at 2000*g* for 5 min at 4°C and immediately processed. Aliquots of 50 μl of plasma were mixed with 3 ml of *tert*-butyl methylether, shaken for 1 min, and centrifuged at 9800*g* for 5 min at 4°C. The organic layer was then transferred to clean tubes and evaporated down at vacuum in an Automatic Environmental Speed Vac evaporator (AES 10, Savant, Barcelona, Spain). This procedure was repeated three times, and the residue was dissolved in 130 μl of physiological saline solution adjusted to pH = 3 and shaken for 1 min. A volume of 100 μl was injected into the High-Performance Liquid Chromatography (HPLC). The chromatographic system consisted of an HPLC Hewlett Packard HP 1100 equipped with an HP1100 quaternary pump, a HP 1100 autosampler, and a fluorescence detector. The excitation and emission λ were 381 and 525 nm, respectively.

The analytical separation was performed at 35°C by a Hypersil BDS-C18 (5-μm particle size) column, preceded by

a C18 precolumn (5-μm particle size). The mobile phase consisted of 0.1 M potassium dihydrogenphosphate (adjusted to pH = 6 with orthophosphoric acid):methanol (75:25) and the flow rate was 0.7 ml/min. The method was linear from 35 to 1000 ng/ml, and the limit of quantification was 10 ng/ml. The precision of the assay method was <5% for three different concentrations, and the accuracy was between 90 and 120% for the same concentrations. The analytical assay was also tested for carboxylate form and under the conditions described before its recovery was negligible.

Data Analysis

All analyses were performed with the first-order conditional estimation method with interaction implemented in the software NONMEM, version V (19). This type of analysis provides estimates of the fixed (typical population) and random (inter-animal and residual variability) parameters. Inter-animal variability (IAV) was exponentially modeled. Differences between observations and model predictions were modeled with a proportional or a combined error model in the case of drug concentrations in plasma or blood cell counts, respectively.

Model selection was based on a number of criteria, such as the exploratory analysis of the goodness-of-fit plots, the estimates and precision of the fixed and random parameters, and the minimum value of the objective function (OBJF) provided by NONMEM. The difference in the OBJF between two hierarchical models was compared with a χ^2 distribution in which a difference of 3.84 points was considered significant at the 5% level.

Pk data were first modeled and then, during the development of the pk/pd model, the individual pk profiles in group II were generated fixing the population model parameters (fixed and random) to those estimated from the animals used to study the kinetics of TPT.

Pk Modeling

TPT disposition into the body was characterized by compartment models. Several classes of absorption models were fitted to the data. The effect of administered dose and time was evaluated on the main disposition and absorption parameters including relative bioavailability.

Pk/Pd Modeling

Data from the three analyzed cellular populations were described separately, and for each of them, observations obtained from the control and treated groups were simultaneously fitted. Figure 2 represents the structure of the model finally selected, which resembles the model recently published by Friberg *et al.* (13). The model can be classified as semiphysiological because it incorporates some of the key and known processes of the cellular cycle. Proliferation and maturation of precursor cells are represented by the first-order rate constant k_{prol} and the mean transition time (MTT), respectively. MTT is reflected in the model as a chain of three transit compartments connected by the first-order rate constant k_{tr}, which value can be derived from the expression (n + 1)/MTT, where n is the number of transit compartments. The model implies that the values of k_{prol} and k_{tr} are the same. Finally, k_{circ} and γ account for the elimination of the circulating cells and the homeostatic regulation, respectively. C_{irc0} is the cell counts at baseline, and drug effects are modeled as a reversible inhibition of k_{prol}. During model selection, a different number of transit compartments, the presence of amplification in the transit chain, inclusion of an effect compartment, differences in the estimates k_{prol} and k_{tr}, zero-order rate of proliferation, reversible E_{MAX} or sigmoidal E_{MAX} and irreversible models accounting for drug effects, or the significance of the homeostatic regulation, was also explored.

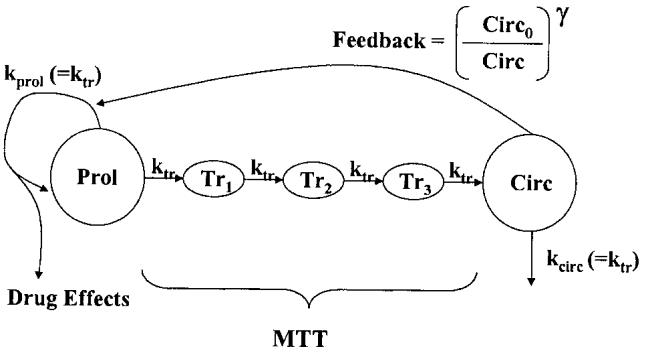

Fig. 2. Schematic representation of the pharmacodynamic model used to describe the hematological effects of TPT.

Statistical Analysis

Group differences in cell counts and body weight at baseline were evaluated by one-way ANOVA test followed by the F test. Within each of the groups II, IIA, and IIB, changes in cell counts and body weight at time to nadir with respect to the time of drug injection were explored by a two-tailed paired Student's *t* test. Statistical significance was set at $p < 0.05$.

RESULTS

General Toxicity and Tumor Growth

Body weight continuously decreased for 7 to 9 days after TPT administration. Groups II, IIA, and IIB showed a maximum reduction in body weight of 18, 19, and 22%, respectively ($p < 0.01$). One rat from group II died on the fourth day during the first cycle of TPT. Severe neutropenia and marked loss of body weight (35%) could be the cause of death.

Figure 3 shows the external mean observed diameters of the tumor measured in all rats. Tumor growth was indistinguishable between untreated and treated animals during the first cycle; however, after the administration of a second TPT dose, tumor size became slightly reduced in comparison with the control group. This reduction was more apparent in rats from group IIB which received a fractionated schedule dosing of TPT (see Fig. 2), nevertheless, these differences were negligible.

Hematology

No statistical differences ($p > 0.05$) were found between control and treated groups in the baseline values of leukocytes (14.5 ± 1.5 vs. 14.6 ± 1.4 10^6/ml), neutrophils (4.42 ± 0.83 vs. 5.1 ± 1.50 10^6/ml), and lymphocytes (4.52 ± 0.84 vs. 4.42 ± 0.50 10^6/ml).

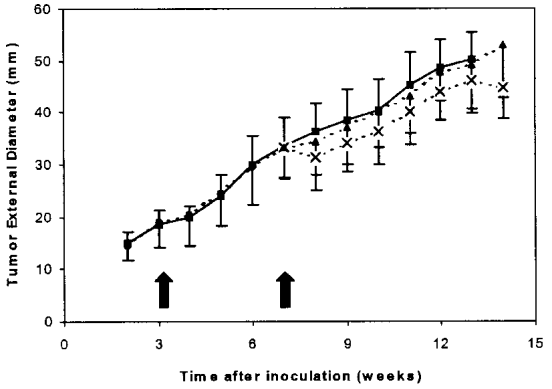

Fig. 3. Results from tumor growth. Symbols from groups I, II, IIA, and IIB corresponding to squares, circles, triangles, and crosses, respectively, represent the mean raw data. Vertical lines show the standard deviation; arrows indicate the times of saline or TPT injections.

Group I showed a significant ($p < 0.01$) increase in leukocyte and neutrophil levels at the end of the measurement time (28 days) with respect to baseline; however, levels of lymphocytes did not statistically change over the time of experiment ($p > 0.05$).

In groups II, IIA, IIB, and for the three studied blood cell populations, nadir occurred at day 3–4 after each TPT injection. The values at nadir were (i) leukocytes 3.18 ± 1.13, 3.64 ± 0.63, 2.90 ± 0.70 10^6/ml; (ii) neutrophils 0.58 ± 0.28, 1.04 ± 0.30, 0.96 ± 0.51 10^6/ml; and (iii) lymphocytes 1.39 ± 0.48, 0.91 ± 0.17, 0.96 ± 0.51 10^6/ml for groups II, IIA, and IIB, respectively. All of these values were significantly ($p < 0.05$) decreased with respect to the corresponding times of drug injection.

Pk Analysis

Disposition of TPT into the body was best described with a two-compartment model. A decrease by 10 points in the OBJF ($p < 0.01$) was found in comparison with the simpler one-compartment model. Drug absorption could be characterized by a first-order process, and no lag time was required. Absorption and disposition processes were not affected by the administered dose or time after tumor cell inoculation ($p > 0.05$). The results could be interpreted as absence of disease effects on systemic kinetic behavior of TPT. Figure 4 shows the observed concentration data vs. time profile and the typical population predictions from the selected model.

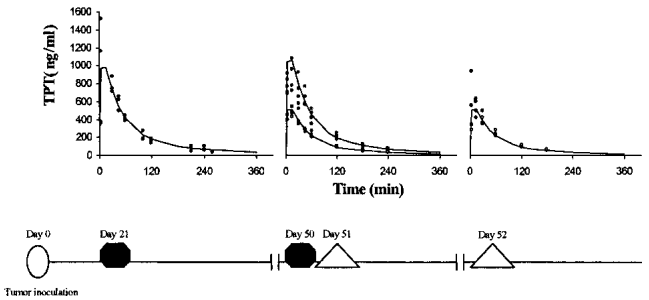

Fig. 4. Pharmacokinetic profiles of TPT. Symbols represent the individual observed plasma concentrations. After the second injection of TPT (days 50 or 51), open circles correspond to group IIB. Solid lines show the typical model predictions.

Table I. Pharmacokinetic Parameter Estimates of TPT in the Rat

Parameter	Estimate	IAV
CL (1/min)	0.022 (0.037)	—
V (1)	1.40 (0.061)	—
CL_D (1/min)	0.010 (0.079)	—
V_T (1)	2.366 (0.051)	—
K_A (1/min)	0.330 (0.114)	32 (0.355)

TPT, topotecan; CL, plasma clearance; V, volume of distribution of the central compartment; CL_D, intercompartmental clearance; V_T, apparent volume of distribution of the peripheral compartment; K_A, first-order rate constant of absorption.
Estimates of inter-animal variability (IAV) are expressed as CV (%). Precision of the estimates is expressed as relative standard error in parenthesis calculated as standard error divided by the parameter estimate.

Estimates of the pk parameters of TPT in the rat are shown in Table I.

Pk/Pd Analysis

Figure 5 shows the entire observed cells vs. time profiles obtained in the studied animals and the typical predictions from the selected model (Fig. 2). Figure 6 shows the individual observed and model predicted cells vs. time profiles for an animal chosen at random. Table II lists the population

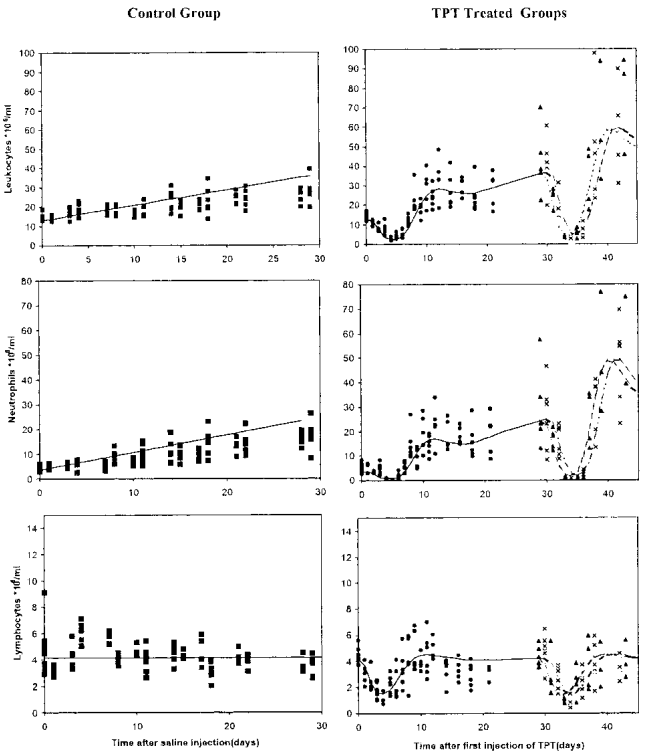

Fig. 5. Time course of hematological effects. Left panels correspond to group I (control) and right panels to TPT-treated groups. Leukocytes, neutrophils, and mature lymphocytes are shown in upper, middle, and lower panels, respectively. Symbols (squares, group I; circles, group II; triangles, group IIA; and crosses, group IIB) represent the observed data and lines the typical model predictions: Solid lines, groups I and II; pointed line, group IIA and dashed line, group IIB.

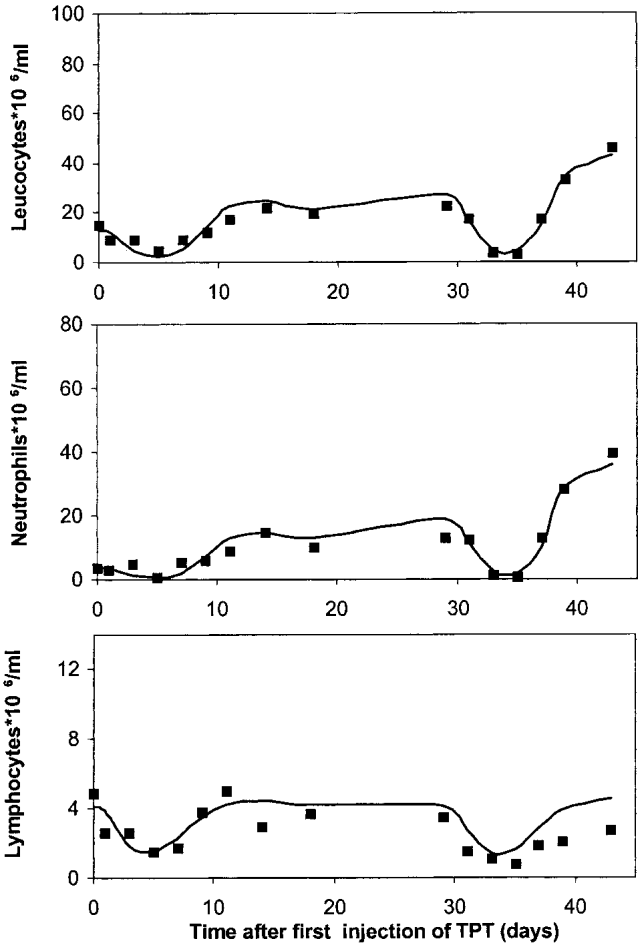

Fig. 6. Individual observations (symbols) and individual model predictions (lines) for an animal chosen at random.

parameter estimates. Typical and individual model prediction and the value of the estimates and their precision confirm the adequacy of the model. It should be noticed that the same structural model, sharing the same parameters (but not the same estimate), was used to describe the kinetics of the three studied cell populations.

Formation of the initial precursors was also modeled with a zero-order rate constant. With this model, parameter precision was very poor and the drug-induced decrease in response was not properly captured. A linear reversible pd model was sufficient to describe drug effects, and when the number of transit compartments was changed or amplification was tested, the fit was not significantly improved ($p > 0.05$). The data did not support different estimates of k_{tr} and k_{circ} ($p > 0.05$). The presence of the rebound phenomenon was found to be statistically significant ($p < 0.05$). The inclusion in the model of a linear time-dependent increase in baseline leukocytes and neutrophils was found to be significant ($p < 0.05$). Other models (i.e., E_{MAX} model) that allow achievement of a new steady-state after cell inoculation were also tried, but the model estimates were meaningless and the predictions were not improved with respect to the linear model. Figure 7 shows the contribution of the parts of the selected model dealing with the time-dependent increase and drug-induced decrease in neutrophils (the same for leukocytes) to the complete model-predicted profiles.

In the model selected for each of the three cell populations, IAV was estimated in MTT and baseline components. Variability in drug effects was not supported by the data ($p > 0.05$).

DISCUSSION

It is well-known that hematotoxicity represents one of the major limitations during chemotherapy treatment, and therefore considerable efforts have been carried out to describe the adverse response vs. drug exposure relationship to improve dose and dose schedule selection. For this particular problem, an evolution from empirical to more physiological models has recently been observed. The value of the AUC has commonly been used to relate drug exposure with a measure of hematological toxicity [i.e., nadir (3,20), or probability to achieve a certain degree of neutropenia (14)]; however, under this approach, description and/or prediction of the time course of hematological toxicity is not possible. Recently, published continuous dynamic models (12,13,21) overcame such limitations and showed that the description of the entire dynamic profile estimating meaningful drug and system-related parameters is possible. In the current work, the time course of the hematological effects of TPT after its administration to tumor-bearing rats has been described using one of the above-mentioned models (13). This study provides novel

Table II. System-Related and Pharmacodynamic Parameters of TPT in the Rat

	Leukocytes		Neutrophils		Lymphocytes	
Parameter	Estimate	IAV	Estimate	IAV	Estimate	IAV
$Circ_0$ ($*10^6$/ml)	14.1 (0.02)	—	4.81 (0.04)	—	4.07 (0.02)	9 (0.6)
MTT (days)	2.18 (0.02)	5.4 (0.54)	2.12 (0.02)	4.4 (0.5)	1.89 (0.08)	8.3 (0.88)
γ	0.18 (0.06)	—	0.18 (0.05)	—	0.16 (0.18)	—
Slp (ml/ng)	0.026 (0.04)	—	0.039 (0.02)	—	0.01 (0.05)	—
Tmp ($*10^6$/day ml)	0.5 (0.15)	53 (0.27)	0.53 (0.11)	53 (0.31)	—	—
Additive error ($*10^6$/ml)	4.41 (0.36)	—	2.41 (0.29)	—	1.08 (0.09)	—
Proportional error	17 (0.12)	—	24 (0.2)	—	—	—

TPT, topotecan; $Circ_0$, absolute cell count at baseline; MTT, mean transit time; γ, parameter controlling the rebound effect; Slp, represents the inhibitory effects of TPT on the rate of synthesis of precursor cells; Tmp, linear relationship time-dependent increase in leukocytes and neutrophils.

Estimates of inter-animal variability (IAV) and proportional error are expressed as CV (%). Precision of the estimates is expressed as relative standard error in parenthesis calculated as standard error divided by the parameter estimate.

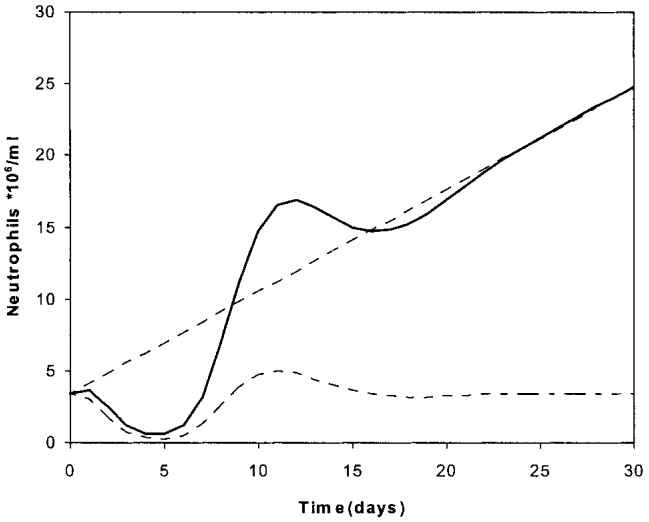

Fig. 7. Contribution of the different parts included in the selected model (solid line) dealing with the time-dependent increase (pointed line) and the decrease in neutrophils induced by TPT (dashed line).

information because (i) the time course of bone marrow suppression of TPT has not yet been described in rats, (ii) the drug was given to rats at an early stage of tumor development, (iii) two entire cycles were completed and different schedule regimens were used, and (iv) the description of the time course of peripheral mature lymphocytes has also been included. The use of this type of preclinical design has recently and repeatedly been suggested to provide useful information about the eventual behavior of chemotherapy agents in humans.

The protocol described by García-Olmo *et al.* (16) was followed to induce tumor growth with very similar results. The DHD/K12-PROb cell line, syngenic with BD-IX rats, is capable of developing a colon adenocarcinoma (16,22). Two recent studies showed that the intramural injection of DHD/K12-PROb cells in the cecum [orthotopic model (22)] or the subcutaneous injection of the same cells into the right side of the chest [heterotopic model (16)] induced tumors that were quantifiable and reproducible. The heterotopic design was chosen in our study because it allowed us to follow disease progression in the same animal. Three weeks after cell injection, saline or TPT dose was administered, as the tumor was large enough to be detected and measured (~18 mm) by macroscopic examination. Although during the second TPT dose administration a slight decrease in the size of tumor was specially observed in group IIB (Fig. 2), drug efficacy was not the aim of the current study.

Pk/pd models in general use the plasma drug concentrations as the driving force for drug effects. Sometimes drug plasma concentrations are not available over the entire duration of the study, and pk information comes from other studies or after the first administration of the drug. In a situation like cancer where a progression of the disease leads to important physiological changes, there is the need to explore if pharmacokinetic behavior remains stable or if on the contrary it is modified with time. Certainly, due to processes of angiogenesis and/or tissue degradation, the pharmacokinetics in the tumor could be changed over time, however, to predict the time course of hematological effects, plasma, or the (non-available) bone marrow kinetics are of greater importance. Our results show that the kinetic behavior of TPT in plasma remains constant in a period of time where the tumor size increases 100% (approximately) (Fig. 2). A comparison with other studies is difficult, but data suggest that the kinetics of TPT in plasma is comparable across strains and species. For example, the estimates of clearance and apparent total volume of distribution found in this study were similar to the ones reported by El-Gizawy *et al.* (23) obtained from Wistar rats.

The final selected model (Fig. 2) has the same structure as the one developed by Friberg *et al.* (13) and used to describe the hematological toxicity of several chemotherapy agents in humans. In the pk/pd field, dealing with indirect response models, usually the formation rate of the studied response is described by a zero-order process that assumes that the amount of precursors is very high and is not affected by the presence of the drug (24). However, a variant of the selected model assuming a zero-order formation of the initial precursors did not capture the main tendencies of the data. In the current model, k_{tr} and k_{circ} are related through MTT, which is not physiologically accurate and has been included in the model as a resource to overcome the time delays in the appearance of cells in the peripheral circulation. It should be taken into account that cell maturation and proliferation can be altered in several physiological and disease states. However, to discriminate between those two parameters, more myelosuppressive regimens and/or measurement of different cell populations within the maturation chain are required.

The selection of the same model to describe the time course of leukocytes and neutrophils (representing the myeloid pathway) and mature lymphocytes is one of the main findings from the modeling exercise. This result is interesting because in most of the articles dealing with the modeling of the hematological toxicity, the lymphoid lineage remains ignored, even though it best reflects the specific immune status of the individual (25,26). Our results show that TPT elicits parallel shifts in the time course of neutrophils and lymphocytes. It has been suggested that chemotherapy develops toxicity by acting over the stem cells (27), therefore similar estimates of Slp would be expected from the analysis of neutrophil and lymphocyte data. In fact, results from the modeling exercise listed in Table 2 show that Slp values are in the same range. The Slp parameter can be used to make comparison between efficacy or toxicity of a drug or a series of compounds.

Estimates of MTT were very similar among the different cell populations. Data in the literature show that in healthy rats, the mean transit time for lymphocytes B and T were around 26 and 18 h, respectively (28), whereas for neutrophils that value is approximately 3 days (12). These values are not very different from the values reported in this study: 2.12 days for neutrophils and 1.89 days for mature lymphocytes (including B and T).

Leukocyte and neutrophil values in the control group showed a significant increase over the time of study that was described with a linear time-dependent model. This effect might be explained by the presence of phagocytes, the first mechanism of the immune system (29), or even by the presence of some stimulating factors (G-CSF; GM-CSF) that seem to be involved in the development of leukocytosis in several types of tumors (30).

Nevertheless, the selected model as it is shown in Fig. 7 had enough resolution to discriminate the drug-induced changes from the drug-independent increase in neutrophils seen in the control group and assumed to be also present in the treated group. In summary, the current study shows the application of a semiphysiological model to describe and predict the hematotoxic effects of TPT, but not its efficacy, in tumor-bearing rats receiving the drug on two occasions and with different dosing schedules.

ACKNOWLEDGMENTS

We kindly acknowledge Dr. D García-Olmo and C.F-.Vega (research unit of Albacete General Hospital, Albacete, Spain) for providing DHD/K12PROb cells and for their help in the animal model. TPT was a generous gift from Smith-Kline Beecham. This work was supported by the Spanish research grants 01/0787 (FISS), SAF2001-1352 (CICYT), and RTIC Cáncer C10/03 (Instituto Carlos III). Cristina Segura was supported by a fellowship from the Government of Navarra. Part of these results were presented at the 2002 AAPS Annual Meeting held in Toronto (Canada).

REFERENCES

1. J. M. Gallo, P. B. Laub, E. K. Rowinsky, L. B. Grochow, and S. D. Baker. Population pharmacokinetic model for topotecan derived from phase I clinical trials. *J. Clin. Oncol.* **18**:2459–2467 (2000).
2. M. L. Rothenberg. Topoisomerase I inhibitors: review and update. *Ann. Oncol.* **8**:837–855 (1997).
3. V. M. Herben, W. W. ten Bokkel Huinink, and J. H. Beijnen. Clinical pharmacokinetics of topotecan. *Clin. Pharmacokinet.* **31**: 85–102 (1996).
4. G. J. Creemers, C. J. H. Gerrits, J. H. M. Schellens, A. S. Planting, M. E. L. van de Burg, V. M. van Beurden, M. de Boer-Dennert, M. Harteveld, W. Loos, I. Hudson, *et al*. Phase II and pharmacologic study of topotecan administered as a 21-day continuous infusion to patients with colorectal cancer. *J. Clin. Oncol.* **149**: 2540–2545 (1996).
5. U. Vanhoefer, A. Harstrick, W. Achterrath, S. Cao, S. Seeber, and Y. M. Rustum. Irinotecan in the treatment of colorectal cancer: clinical overview. *J. Clin. Oncol.* **19**:1501–1518 (2001).
6. J. Bennouna and J. Y. Douillard. Therapeutic strategies for colorectal cancer in Europe and the United States: focus on chemotherapy for advanced colorectal cancer. *Int J Clin Oncol.* **7**: 236–244 (2002).
7. R. Garcia-Carbonero. and J. G. Supko. Current perspectives on the clinical experience, pharmacology and continued development of the Camptothecins. *Clin. Cancer Res.* **8**:641–661 (2002).
8. J. J. Liu, R. L. Hong, W. F. Cheng, K. Hong, F. H. Chang, and Y. L. Tseng. Simple and efficient liposomal encapsulation of topotecan by ammonium sulfate gradient: stability, pharmacokinetic and therapeutic evaluation. *Anticancer Drugs* **13**:709–717 (2002).
9. E. K. Rowinsky. Weekly topotecan: an alternative to topotecan's standard daily x 5 schedule? *Oncologist* **7**:324–330 (2002).
10. L. Brynne, L. K. Paalzow, and M. O. Karlsson. Mechanism-based modeling of rebound tachycardia after chronic /-propanolol infusion on spontaneous hypertensive rats. *J. Pharmacol. Exp. Ther.* **290**:664–671 (1999).
11. M. J. Garrido, M. Valle, M. A. Campanero, R. Calvo, and I. F. Trocóniz. Modeling of the in vivo anitnociceptive interaction between an opioid agonist, (+)-*O*-desmethyltramadol, and a monoamine reuptake inhbitor, (–)-*O*-desmethyltramadol, in rats. *J. Pharmacol. Exp. Ther.* **295**:352–359 (2000).
12. L. E. Friberg, A. Freijs, M. Sandstrom, and M. O. Karlsson. Semiphysiological model for the time course of leukocytes after varying schedules of 5-fluorouracil in rats. *J. Pharmacol. Exp. Ther.* **295**:734–740 (2000).
13. L. E. Friberg, A. Henningsson, H. Maas, L. Nguyen, and M. O. Karlsson. Model of chemotherapy-induced myelosuppression with parameter consistency across drugs. *J. Clin. Oncol.* **20**:4713–4721 (2002).
14. D. R. Mould, N. H. Holford, J. H. Schellens, J. H. Beijnen, P. R. Hutson, H. Rosing, W. W. ten Bokkel Huinink, E. K. Rowinsky, J. H. Schiller, M. Russo, and G. Ross. Population pharmacokinetic and adverse event analysis of topotecan in patients with solid tumours. *Clin. Pharmacol. Ther.* **71**:334–348 (2002).
15. U. C. Nygaard and M. Løvik. Blood and spleen lymphocytes as targets for immunotoxic effects in the rat—a comparison. *Toxicology* **174**:153–161 (2002).
16. D. C. Garcia-Olmo, H. H. Riese, J. Escribano, J. Ontanon, J. A. Fernandez, M. Atienzar, and D. Garcia-Olmo. Effects of long-term treatment of colon adenocarcinoma with crocin, a carotenoid from saffron (Crocus sativus L.): an experimental study in the rat. *Nutr. Cancer* **35**:120–126 (1999).
17. K. Hettiarachchi, C. E. Green, S. Ramanathan-Girish, B. Wu, C. J. Jackson, S. Ridge, M. A. Salem, and M. E. Lanser. Analysis of 2beta-carbomethoxy-3beta-(4-fluorophenyl)-N-(3-iodo-E-allyl)nortropane in rat plasma. II. Pharmacokinetic profile in male and female Sprague-Dawley rats evaluated by capillary electrophoresis. *J. Chromatogr. A* **924**:471–481 (2001).
18. A. L. Landay and K. A. Muirhead. Procedural guidelines for performing immunophenotyping by flow cytometry. *Clin. Immunol. Immunopathol.* **52**:48–60 (1989).
19. S. L. Beal. and L.B. Sheiner (eds.) *NONMEM Users Guides*. NONMEM Project Group, University of California at San Francisco, San Francisco, CA (1992).
20. D. I. Jodrell, M. J. Egorin, R. M. Canetta, P. Langenberg, E. P. Goldbloom, J. N. Burroughs, J. L. Goodlow, S. Tan, and E. Wiltshaw. Relationships between carboplatin exposure and tumor response and toxicity in patients with ovarian cancer. *J. Clin. Oncol.* **10**:520–528 (1992).
21. M. O. Karlsson, V. Molnar, J. Bergh, A. Freijs, and R. Larsson. A general model for time-dissociated pharmacokinetic-pharmacodynamic relationship exemplified by paclitaxel. *Clin. Pharmacol. Ther.* **63**:11–25 (1998).
22. D. Garcia-Olmo, M. Garcia-Rivas, D. C. Garcia-Olmo, and M. Atienzar. Orthotopic implantation of colon carcinoma cells provides an experimental model in the rat that replicates the regional spreading pattern of human colorectal cancer. *Cancer Lett.* **132**: 127–133 (1998).
23. S. A. El-Gizawy and M. A. Hedaya. Comparative brain tissue distribution of camptothecin and topotecan in the rat. *Cancer Chemother. Pharmacol.* **43**:364–370 (1999).
24. N. L. Dayneka, V. Garg, and W. J. Jusko. Comparison of four basic models of indirect pharmacodynamic responses. *J. Pharmacokinet. Biopharm.* **21**:457–478 (1993).
25. C. L. Mackall, T. A. Fleisher, M. R. Brown, I. T. Magrath, A. T. Shad, M. E. Horowitz, L. H. Wexler, M. A. Adde, L. L. McClure, and R. E. Gress. Lymphocyte depletion during treatment with intensive chemotherapy for cancer. *Blood* **84**:2221–2228 (1994).
26. A. K. Nowak, B. W. Robinson, and R. A. Lake. Gemcitabine exerts a selective effect on the humoral immune response: implications for combination chemo-immunotherapy. *Cancer Res.* **62**: 2353–2358 (2002).
27. M. Ogawa. Differentiation and proliferation of hematopoietic stem cells. *Blood* **81**:2844–2853 (1993).
28. J. Westermann, Z. Puskas, and R. Pabst. Blood transit and recirculation kinetics of lymphocyte subsets in normal rats. *Scand. J. Immunol.* **28**:203–210 (1988).
29. L. A. Segel and I. R. Cohen. *Design Principles for the Immune System and Other Distributed Autonomous Systems*, Oxford University Press, New York, 2001.
30. K. Kojima. F. Nakashima, A. Boku, Y. Muroishi, I. Nakanishi, and Y. Oda. Clinicopathological study of involvement of granulocyte colony stimulating factor and granulocyte-macrophage colony stimulating factor in non-lymphohematopoietic malignant tumors accompanied by leukocytosis. *Histol. Histopathol.* **14**: 1005–1016 (2002).